HKIE THE HONG KONG INSTITUTION OF ENGINEERS 香港工程師學會

Class A Prediction Symposium on Debris Flow Impact Forces on Single and Dual Barriers

Charles W W Ng[1], Clarence E Choi[2], Haiming Liu[1], Sunil Poudyal[1], Aastha Bhatta[1], W A Roanga K De Silva[1] and Raymond W M Cheung[3]

[1] Department of Civil and Environmental Engineering, The Hong Kong University of Science and Technology, Hong Kong, People's Republic of China
[2] Department of Civil Engineering, The University of Hong Kong, Hong Kong, People's Republic of China
[3] Geotechnical Engineering Office, Civil Engineering and Development Department, the HKSAR Government, People's Republic of China

ABSTRACT

Over recent years, significant advances have been made in the modelling of the impact dynamics between debris flows and single and dual rigid and flexible barriers. Numerical tools and analytical formulations have been proposed to predict the impact force, runup height, barrier deformation, and overflow and landing dynamics. However, there remains a dearth of well-recognised tools that can be used in routine engineering design practice because their reliability is unclear. On 8 and 9 May 2022, a virtual Class A Prediction Symposium on Debris Flow Impact Forces on Single and Dual Barriers was held to evaluate the reliability of existing design tools and identify areas for improvement to advance the current state of barrier design. The symposium was organised by The Hong Kong University of Science and Technology, Norwegian University of Science and Technology, Institute of Mountain Hazards and Environment of the Chinese Academy of Sciences, and the Geotechnical Engineering Office of the Civil Engineering and Development Department of the HKSAR Government. This paper summarises the existing research on flow-barrier interaction, and details of the symposium, including the prediction cases and results, roundtable discussion, and future research directions.

KEYWORDS Debris flow; Class A prediction; numerical; dual barriers; flow-barrier interaction; impact
CONTACT Clarence E Choi cechoi@hku.hk
Received 14 July 2022

1. Background

With climate change causing an increase in the frequency of extreme rainfall events and urbanisation leading to encroachment onto natural hillsides, the threat posed by landslides is expected to increase (Cui et al., 2019; Stoffel et al., 2014). Among the different types of landslides, debris flows are the most dangerous. These large discharges of soil and water have been reported to damage infrastructure and have buried entire settlements (e.g., 2010 debris flow in Zhouqu, China, caused about 1,700 fatalities (Ren, 2014)). If sustainable development is to succeed in mountainous regions, scientists and engineers will need to design robust and cost-effective engineering solutions to arrest debris flows.

The most commonly used engineering solutions for debris flow hazard mitigation are reinforced concrete rigid barriers (Hübl and Fiebiger, 2005) and flexible steel net barriers (Wendeler et al., 2008). To arrest large debris flow volumes, a single barrier may not have sufficient retention capacity. Therefore, a series of rigid or flexible barriers (Hübl and Fiebiger, 2005; SWCB, 2019) may be installed along a drainage line to create a cascading effect to progressively impede and retain a debris flow. The key to optimising the design of a multiple barrier system is to predict the impact force (Faug, 2020; Kwan, 2012; NILIM, 2016), barrier deformation if any, runup height (Choi et al., 2015; Fang et al., 2022; Iverson et al., 2016), overflow and landing angles (Ng et al., 2018, 2022), and impact force on the next barrier in succession (Ng et al., 2021a). By revealing these design parameters, the spacing between barriers and the individual height of each barrier can be designed. However, advanced numerical and analytical tools are required to predict the design parameters for such a complex debris flow-structure interaction problem. The reliability of existing tools for predicting the required design variables remains poorly understood.

Predictions in geotechnical engineering can be classified into three classes (Lambe, 1973). Class A predictions are made before an event has occurred. Class B predictions are made during an event with some data during the initial stages of the process. The outcome of an event being predicted may be unknown (Class B) or known (Class Bl). Class C predictions are made after an event has occurred. Most engineering decisions and actions are based on Class A predictions and sometimes on Class B predictions. However, most evaluations of design tools and prediction techniques are based on Class C1 predictions. This is because the back-analysis of field data is useful for identifying the underlying mechanisms of complex geotechnical engineering problems (Lambe, 1973), such as debris flow-barrier interaction. However, engineers must be cautious when using Class C1 predictions to prove the validity of any prediction tool or technique. A

lucky engineer can still misuse theory to make a correct prediction. Moreover, Class C1 predictions may be inadequate to assess the performance of a prediction tool because the need to obtain a "good match" with results often masks the judgement decisions made at each stage of the process. More importantly, the success or failure of Class C1 predictions may only be relevant for a unique field case, which does not permit a conclusive evaluation of a prediction tool or technique. Class B predictions are less helpful for debris flow hazard mitigation, which must be conducted before an event to protect downstream facilities. Class A predictions are the most useful because they help to understand the reliability of the existing tools for debris flow hazard mitigation. Table 1 gives a summary of the different types of predictions.

Table 1. Classification of predictions (Lambe, 1973).

Prediction class	When the prediction is made	Results at the time the prediction is made
A	Before event	-
B	During event	Not known
B1	During event	Known
C	After event	Not known
C1	After event	Known

To carry out a holistic assessment of the existing capabilities of design tools for predictions of the impact dynamics of debris flow on barriers, a Class A prediction symposium was held virtually on 8 and 9 May 2022. The test setup, test programme and procedures were provided to the participants to make Class A predictions. Physical tests of debris flow impacting single and dual rigid and flexible barriers were carried out using a 28-m-long field-scale flume. The predicted results were then compared with the measured physical test results. A roundtable discussion with local and international experts was held to identify areas for advancement. A summary of the symposium programme and round-table panellists is given in Table 2.

Table 2. Symposium programme.

Time (GMT+8)	Description
Day 1: 8 May 2022 *Moderator: Charles Ng*	
9:00 to 9:05	**Opening remarks** *By Charles Ng*
9:05 to 9:50	**Keynote lecture 1: On numerical simulation of debris flow: it's all about material behaviour** *By Wei Wu*
9:50 to 10:35	**Keynote lecture 2: Mechanisms and consequences of fast rainfall-induced landslides: the experience gained in Campania Region, Italy** *By Luciano Picarelli*
10:35 to 11:00	**Break**
11:00 to 11:25	**Presentation of physical test results** *By Sunil Poudyal*
11:25 to 11:55	**Presentation of results and announcement of winners** *By Clarence Choi*
	Presentation of awards *By Ringo Yu*
12:00 to 12:40	**Presentation by winners**
12:40 to 12:45	**Closing remarks** *By Charles Ng*
Day 2: 9 May 2022 *Moderator: Raymond Cheung*	
9:00 to 9:05	**Opening remarks** *By Raymond Cheung*
9:05 to 9:50	**Keynote lecture 3: Introducing emerging technologies for slope safety** *By Kenichi Soga*
9:50 to 10:35	**Keynote lecture 4: Grain flows over wall-like obstacles: induced patterns and impact forces** *By Thierry Faug*
10:35 to 11:00	**Break**
11:00 to 12:30	**Roundtable discussion** *By Raymond Cheung, Clarence Choi, Thierry Faug, James Sze, Johnny Cheuk, Thomas Hui, C K Lau and Sabatino Cuomo*
12:30 to 12:45	**Closing remarks** *By Charles Ng*

This paper provides a summary of the existing state of research on debris flow-barrier interaction, prediction cases, assessment criteria, prediction results, and roundtable discussion.

2. Existing state of research

2.1. Impact force

In existing design guidelines, the impact force exerted by debris flows on barriers is predicted using hydrostatic and hydrodynamic impact models. In the hydrostatic model, the debris impact pressure on a barrier is calculated as follows:

$$p_{\mathrm{d}} = k\rho g h \,, \tag{1}$$

where p_d is the impact pressure (N/m^2), k is the static pressure coefficient (dimensionless), ρ is the bulk density

of the debris (kg/m^3), g is the gravitational acceleration (m/s^2), and h is the flow depth of the impacting debris (m). Equation (1) is commonly used for practical design because only the bulk density and impacting flow depth of the debris are required (Hübl et al., 2009; Proske et al., 2011; Vagnon and Segalini, 2016). Equation (1) is simple; however, as reported by Vagnon (2020), the hydrostatic model may only apply to low-velocity debris flows on shallow slopes.

As an alternative to the hydrostatic model, the hydrodynamic equation can be used to estimate the dynamic debris impact pressure:

$$p_{\mathrm{d}} = \alpha \rho v^2 , \tag{2}$$

where α is the dynamic pressure coefficient (dimensionless), and v is the velocity of the impacting debris (m/s). An additional $\sin\theta$ term is introduced in Equation (2) in the design guidelines pertaining to Hong Kong (Kwan, 2012) and mainland China (CAGHP, 2018; MLR, 2006) to consider the different impact angles θ with respect to the flow direction and force-bearing surface. Equation (2) is applicable in practice because it only requires the bulk density and velocity of the impacting debris and an empirical coefficient. The derivation of the equation is based on conservation of linear momentum, borrowed from hydraulics for estimating the impact force on vanes by water jets (Chadwick and Morfett, 1986). However, debris flows are in reality much more complex than the scenario of an incompressible water jet impacting a vane.

This dynamic pressure coefficient has been extensively studied by researchers using experimental, analytical, and numerical approaches, and a range of values have been reported. Proske et al. (2011) back-analysed eight field cases and reported that the dynamic pressure coefficient ranged from 0.38 to 18.76. Moreover, the dynamic pressure coefficient values differ across design guidelines for different regions. In Taiwan (SWCB, 2019), the coefficient is recommended to be from 0.5 to 2.0 for a rigid barrier. In the early versions of the design guidelines in Hong Kong, this coefficient was specified as 2.0 and 2.5 for flexible (Kwan and Cheung, 2012) and rigid (Kwan, 2012) barriers, respectively. These recommended dynamic pressure coefficients implicitly allow for the presence of particles smaller than 0.5 m (Kwan et al., 2018). Flexible barriers typically correspond to a lower dynamic pressure coefficient than those of rigid barriers because of their deformable and pervious nature that allows certain debris to pass through upon impact. Wendeler (2008) conducted laboratory-scale experiments and recommended dynamic pressure coefficients ranging from 0.7 to 2.0 for the design of flexible barriers. Recently, the dynamic pressure coefficient for the design of rigid barriers in Hong Kong was decreased from 2.5 to 1.5 (GEO, 2020). In Austria (ASI, 2013) and Japan (NILIM, 2016), the dynamic pressure coefficient is set as unity for designing rigid barriers.

Several researchers have proposed impact models based on regression analyses (Hübl and Holzinger, 2003; Hübl et al., 2009), in which experimental and field measurements are scaled using the Froude number ($Fr = v/\sqrt{gh}$). Ng et al. (2021a) proposed a modified approach to calculating peak impact force for dual rigid and flexible barriers by combining hydrostatic and hydrodynamic approaches:

$$F_{\mathrm{peak}} = 0.5 k \rho g h^2 w \left(1 + \frac{2\alpha}{k} Fr^2\right), \tag{3}$$

where, $k = 1$, and $\alpha = \begin{cases} 1.5, & \text{first rigid barrier} \\ 1.0, & \text{second rigid barrier} \\ 1.0, & \text{first flexible barrier} \\ 1.0, & \text{second flexible barrier} \end{cases}$

Equation (3) is an improvement in physics over Equations (1) and (2). Equation (3) explicitly accounts for dynamic and static components of load, whereas Equation (1) only accounts for the dynamic load implicitly and Equation (2) only accounts for the static load implicitly. This semi-empirical formulation recommended dynamic and static pressure coefficients determined from dry sand, water, and debris flow impact data in the literature. The data include test results from laboratory scale to field scale (i.e., Kadoorie Centre). Details are described in Ng et al. (2021a). Based on these benchmark conditions, (i) $\alpha = 1.5$ and $k = 1$ for the first rigid barrier, and (ii) $\alpha = 1$ and $k = 1$ for the second rigid barrier and dual flexible barriers provides conservative estimates for debris flow impact.

2.2. Runup height

Debris flow impact on rigid and flexible barriers results in runup along the load-bearing barrier surface and over-spill. The prevailing runup mechanism is dependent on the flow type and Froude number before impact. The energy balance method (Choi et al., 2015) and momentum conservation method (Iverson et al., 2016; Johannesson et al., 2009) are the two commonly used methods to predict the runup height in design guidelines (Kwan, 2012).

The runup height (h_{r}) calculated using the energy balance method is as follows:

$$h_{\mathrm{r}} = h + \frac{v^2}{2g\cos\theta} , \tag{4}$$

where θ is the slope angle. Equation (4) provides a conservative h_{r} as the energy loss during runup mechanism is neglected. The debris flow is considered as a point mass in which the momentum flux from the entire flow mass pushing the flow front upwards is not considered. In comparison, the momentum conservation method considers the mass and momentum conservation for the reflected

shock that occurs at barrier impact (Kwan, 2012) and is given as follows:

$$\frac{\rho_f}{\rho}\left(\frac{h_r}{h}\right)^2 - \frac{h_r}{h} - 1 + \left(\frac{\rho_f h_r}{\rho h}\right)^{-1} - 2\,\frac{v^2}{gh} = 0\,, \qquad (5)$$

where ρ_f is the density of the debris in contact with the barrier surface. The energy balance method is more suitable for fluidised biphasic flows while the momentum conservation method is more suitable for dry granular flows (Choi et al., 2015; GEO, 2020).

2.3. Multiple barrier design

Instead of erecting a large terminal barrier by adopting a series of smaller barriers along a flow path, a cascading effect can be generated to progressively retain and decelerate debris flows (Ng et al., 2018; Takahashi, 2014). In the design of such multiple barriers, the spacing between barriers can be estimated to maximise the storage capacity of debris material (VanDine, 1996) or by considering the flow impact dynamics (Ng et al., 2021a). The method by VanDine (1996) recommends a minimum barrier spacing (L_{min}) solely based on the maximum retained volume and is used in the existing guidelines (CGS, 2004; NILIM, 2007). However, this method does not consider the interaction mechanism between the flow and barrier resulting in underestimations of the spacing required (Ng et al., 2022).

The multiple barriers should be spaced so that overflow impacts the channel to maximise energy dissipation before impacting the next barrier. To design for overflow, the launch angle and maximum overflow distance are required. The analytical approach proposed by Ng et al. (2021a) to predict the horizontal overflow distance (x_i) is given as follows:

$$x_i = \frac{v_m^2}{g}\left[\tan\theta + \sqrt{\tan^2\theta + \frac{2gB}{v_m^2}}\right], \qquad (6)$$

where v_m is overflow velocity and B is the barrier height. Equation (6) implicitly assumes that the overflow is horizontal from the barrier crest. The calculated overflow distance from Equation (6) provides a minimum design spacing between barriers. The overflow velocity (v_m) is calculated by reducing potential energy loss when debris runs up to the barrier crest as follows:

$$v_m = \sqrt{v^2 - 2g\cos\theta\, B}\,, \qquad (7)$$

Furthermore, the landing angle with respect to the channel bed governs flow velocity after landing. The smaller the landing angle, the larger will be the downstream velocity. Ng et al. (2021a) provides comprehensive details of a multiple barrier design framework, including the calculation of landing velocity.

2.4. Full-scale certification of flexible barriers

The design of flexible barriers for rock fall protection requires barriers to be certified using full-scale tests in compliance with ETAG027:2013, which has been superseded by EAD 340059-00-016:2018. Rock fall barriers are rated based on the impact energy that they can withstand (Geobrugg, 2012; Maccaferri, 2021; Trumer, 2015). The impact energy of a discrete boulder is simple to characterise (i.e., for free fall the kinetic energy at impact is equal to its potential energy). Certification tests for rockfall protection only require that a barrier brings a boulder with specified impact energy to rest even if some structural components of the barrier yield or fail. Designers can then use these tested barriers as standardised ones that can resist a specific energy level without the need for complex calculation design procedures. In contrast to rock fall impact, debris flow loading is more complex because of its surge-like nature, hard inclusions, and simultaneous static and dynamic contributions. More importantly, debris flow dynamics are scale-dependent, so the largest feasible facilities are required to simulate them (Iverson, 2015). Such facilities do not yet exist. As such, there are currently no certification tests or standardisation of flexible barriers for resisting debris flows. Consequently, flexible barriers for debris flow require complex design procedures that may be overdesigned. Evidently, some form of standardised testing would help to streamline the design process for debris flow resisting flexible barriers.

2.5. Numerical tools for modelling debris flow

Most well-established numerical methods used to model debris flow are grid-based, such as the finite element or finite volume methods. However, the use of grid-based methods involves the challenges related to mesh distortion when large deformations are simulated. An alternative to traditional grid-based numerical methods is continuum-based particle methods (Soga et al., 2016), which offer the potential for solving field-scale applications involving large deformation of geomaterials. Among existing continuum-based particle methods, Smooth Particle Hydrodynamics (SPH) (Gingold and Monaghan, 1977; Lucy, 1977), Particle Finite Element Method (PFEM) (Larese et al., 2008) and Material Point Method (MPM) (Soga et al., 2016) have been gaining traction for solving large deformation problems. These particle-based methods have been successfully applied to solve geotechnical problems, including granular materials (Bui et al., 2008; Dávalos et al., 2015; Dunatunga and Kamrin, 2015), debris flows (Cuomo et al., 2021; Pastor et al., 2009; Wang et al., 2022), slope failure (Bui et al., 2011; Jin et al., 2022; Soga et al., 2016), and barrier impact problems (Cuomo et al., 2021; Ng et al., 2020).

Debris flow dynamics are governed by pore pressure changes (Iverson et al., 2005). However, the bulk of existing models in the literature neglect the solid-fluid interaction,

which leads to changes in pore pressures. Additionally, most practical debris flow models rely on depth-averaged (i.e., quasi-2D) formulations for computational efficiency. In reality, debris flow impact is an unsteady 3D process, especially flexible barrier impact, with obvious momentum exchange between the flow and the structure. Such scenarios render depth-averaged assumptions invalid.

Recently, numerical simulations that explicitly consider the biphasic nature of debris flows have been developed. These tools include the coupled computational fluid mechanics-discrete element method (CFD-DEM), which has been used to simulate the impact of debris flows on rigid and flexible barriers (Li et al., 2020; Leonardi et al., 2016) and coupled biphasic SPH or MPM models used to model the impact on rigid barriers (Cuomo et al., 2021; Dai et al., 2017). Some of these models have relaxed depth-averaged assumptions but assume a plane-strain approximation in modelling debris flow impact on rigid and flexible barriers (Cuomo et al., 2021; Dai et al., 2017). Notwithstanding this, coupled models have not yet been systematically evaluated because dynamic pore pressure changes in debris flows are difficult to replicate and measure. Therefore, it remains unclear whether the constitutive behaviour for coupled models is physically correct. In addition, the effects of larger boulders are usually neglected in existing models. Boulders have profound effects on the prevailing impact dynamics (GEO, 2020). Furthermore, rigid, and smooth boundaries are often adopted in lieu of erodible ones, which can be entrained to increase the momentum of a debris flow.

3. Details of the prediction exercise

3.1. Field-scale flume experiments

The largest feasible facilities are required to replicate the prototype dynamics of debris flows because of disproportionate timescale for pore pressure diffusion and contribution of viscous stresses from lab-scale models (Iverson, 2015). Therefore, an existing field-scale model in Hong Kong (Figure 1) is used to generate high-fidelity measurements to compare the results from the prediction cases. The flume model has a storage compartment that can hold 10 m^3 of debris. A double gate system is used to retain the debris from the storage compartment. The bed of the storage compartment is inclined at 30°. Downstream from the storage compartment is a channel with a length of 15 m inclined at 20°. At the mouth of the inclined channel, there is a horizontal channelised runout section with the same width as the inclined channel and 4.2 m in length. At the end of the runout section, model barriers are installed.

Figure 1. 28-m-long flume at Kadoorie Centre in Hong Kong.

3.1.1. Instrumentation

Instrumentation cells are installed on the channel bed. Each cell measures basal normal and shear stresses using load cells and pore pressure changes using transducers. Laser displacement sensors are mounted above each cell to measure the flow depth. The normal stress combined with the flow depth is used to estimate the bulk density. An unmanned aerial vehicle (UAV) is deployed above the flume to capture the flow kinematics. Additionally, high-speed cameras are mounted around the model barriers to capture the impact kinematics.

3.1.2. Barrier configurations

The interaction between debris flow and dual rigid and flexible debris resisting barriers is modelled. A debris flow volume of 9.0 m^3 is modelled for each test. Details of the barrier configurations modelled using the field-scale flume are summarised in Table 3.

Table 3. Test programme.

Case	First barrier	Second barrier
Rigid barrier	• Size: 1.95 m wide x 0.80 m high • 20 mm thick Al6061 plate with reinforcement • A load cell at each corner	• Size: 1.95 m wide x 1.50 m high • Reinforced L-shaped concrete barrier with 20 mm steel front plate • A load cell at each corner (Ng et al., 2021b)
Flexible barrier	• Size: 2.00 m x 0.80 m • 100 mm diameter ring net mesh panel • 25 mm square opening secondary mesh • Two 16 mm diameter steel wire rope supporting cables • No brake elements • A load cell per cable	• Size: 4.00 m x 1.50 m • 200 mm diameter ring net mesh panel • 6 mm square opening secondary mesh • Three 16 mm diameter steel wire rope supporting cables • A brake element per cable • A load cell per cable

3.1.3. Model barriers

Figure 2 shows a side elevation view of the dual rigid barrier model setup and instrumentation layout. The first rigid barrier is 0.80 m high and 2 m wide and is installed at a distance of 6.0 m downstream from the gate. The first rigid barrier is modelled as an aluminium plate supported by load cells at each corner. The second rigid barrier is 1.5 m tall and 2 m wide and is installed at a distance of 19.2 m downstream from the gate in the runout section. The second rigid barrier is an L-shaped reinforced concrete wall with a 20 mm thick steel plate mounted in front of it. Load cells are sandwiched at each corner between the steel plate and concrete wall.

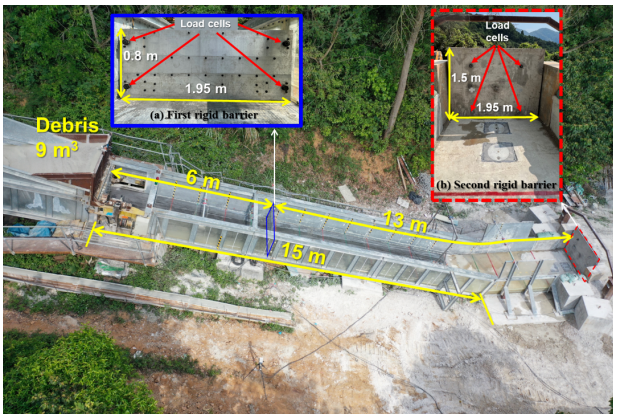

Figure 2. Dual rigid barrier model setup in the 28 m-long flume (inset (a) shows details of the first model rigid barrier; and inset (b) shows the second model rigid barrier).

Figure 3 shows details of the dual flexible barrier model setup. Figure 3(a) shows the first model flexible barrier, which is made of a net panel of high-strength steel rings that are 100 mm diameter rings. The first flexible barrier is supported by two steel wire rope cables that are 16 mm in diameter. Each cable is anchored to the side walls of the flume. Load cells are used to measure the axial load on each cable. A secondary mesh with 25 mm openings is used to cover the ring net panel to retain coarse debris material during impact. Figure 3(b) shows details of the second model flexible barrier. The second model flexible barrier is installed in the runout section and is 4.0 m wide. It has a net panel with 200 mm diameter rings. The panel is supported by three steel wire rope cables with a diameter of 16 mm. A brake element is installed on each main cable and the ends of the cables are anchored to a steel portal frame.

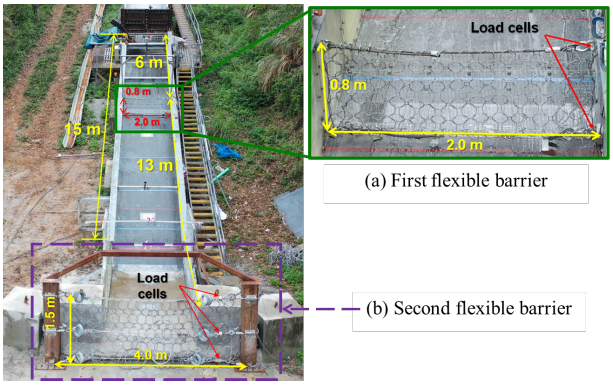

Figure 3. Dual flexible barriers model setup in the 28 m-long flume (a) first flexible barrier; and (b) second flexible barrier.

3.1.4. Modelling procedures

The model barriers and instrumentation are installed in the flume. A premixed volume of 9 m^3 of debris material is prepared and placed into the storage container. The gate is then opened to initiate dam-break flow and to release the debris down the inclined channel. The debris accelerates downstream and impacts the model barriers. Data are sampled by a high-speed data logger. Concurrently, videos are captured from the UAV-mounted cameras and high-speed cameras. At the end of the impact test, the deformation of the flexible barriers and deposition profile of the debris material are measured.

3.2. Assessment criteria

The prediction cases are categorised as rigid or flexible barriers and single or dual barriers. The rationale behind the assessment criteria for the single barriers is that if the flow depth and velocity predictions before impacting a barrier are not close to the measured ones, then it is unlikely that the prevailing impact force and runup height predictions would be close as well. Furthermore, in order for the impact force and runup predictions on the second barrier to be close to measured results, then the overflow distance and landing angle from the first barrier need to be close to the measured ones. Lastly, a higher weighting factor is given to the predictions of the impact dynamics on

Table 4. Details of assessment criteria.

Barrier type	Single/Dual	Parameter	Unit	Mark	Weighting factor
Rigid	Single	Flow depth	M	30	0.4
		Flow velocity	m/s	30	
		Peak impact force	kN	30	
		Maximum runup height	M	10	
		Total		100	
	Dual	First rigid barrier			
		Maximum overflow distance	M	30	
		Flow front landing angle	Deg	30	
		Second rigid barrier			
		Peak impact force	kN	30	
		Maximum runup height	M	10	
		Total		100	
Flexible	Single	Flow depth	M	30	0.6
		Flow velocity	m/s	30	
		Peak impact force	kN	30	
		Maximum barrier deflection	M	10	
		Total		100	
	Dual	First flexible barrier			
		Maximum overflow distance	M	30	
		Flow front landing angle	Deg	30	
		Second flexible barrier			
		Peak impact force	kN	30	
		Maximum runup height	M	10	
		Total		100	

Table 5. Participating teams and adopted prediction methods.

Team	Model	2D/ 3D	References
1[a]	ALE finite-element method (LS-DYNA)	3D	Kwan et al. (2019, 2021)
2[b]	Discrete element method (ROCKY)	3D	Hofmann and Berger (2022)
3[c]	ALE finite-element method (LS-DYNA)	3D	Kwan et al. (2019, 2021)
4[d]	Nodal particle finite-element method (PFEM) and analytical formulation	2D	Tan et al. (2020)
5[e]	Continuum (particle-based) SPH	2D	Peng et al. (2017, 2019)
6[f]	LS-DYNA for incoming flow and analytical formulation for impact	3D	Song et al. (2019, 2021); Faug et al. (2012, 2015); Wang et al. (2022); Kwan et al. (2015); Hungr and McClung (1987)
7[g]	Continuum (particle-based) SPH	2D	Peng et al. (2019, 2022)
8[h]	Continuum (particle-based) MPM	2D	Cuomo et al. (2021); Di Perna et al. (2022); Martinelli and Galavi (2022)
9[i]	Continuum (particle-based) SPH	2D	Huang et al. (2012); Zhang et al. (2016)

a Ryan Tse, James Law, Arthur Cheung and Jack Yiu from Ove Arup and Partners Hong Kong Ltd., Hong Kong, People's Republic of China
b Simon Berger and Robert Hofmann from Unit of Geotechnics, Faculty of Engineering Sciences, University of Innsbruck, Austria
c Max K H Ma, Jonathan W C Lau, Harris W K Lam and Thomas K C Wong from Geotechnical Engineering Office, Civil Engineering and Development Department, Hong Kong, People's Republic of China
d Dao-Yuan Tan, Lu-Jia Yu, Zhen-Yu Yin, Jian-Hua Yin and Yin-Fu Jin from Department of Civil and Environmental Engineering, The Hong Kong Polytechnic University, Hong Kong, People's Republic of China; Jian-Fei Chen from Department of Ocean Science and Engineering, The Southern University of Science and Technology, People's Republic of China
e Chengwei Zhu, Yadong Wang and Wei Wu from the Institute of Geotechnical Engineering (IGT) of the University of Natural Resources and Life Sciences, Vienna, Austria; Chong Peng from ESS Engineering Software Steyr GmbH, Austria
f Dongri Song, Gordon G D Zhou and Xiaoqing Chen from Institute of Mountain Hazards and Environment, Chinese Academy of Sciences, Chengdu, China; Ruiwang Yu from Shenzhen Urban Transport Planning Center Co., Ltd, Shenzhen, People's Republic of China
g Yadong Wang from the Institute of Geotechnical Engineering (IGT) of the University of Natural Resources and Life Sciences, Vienna, Austria
h Sabatino Cuomo and Angela Di Perna from Geotechnical Engineering Group (GEG), University of Salerno, Italy; Mario Martinelli from Deltares, Delft, the Netherlands
i Weijie Zhang from College of Civil and Transportation Engineering, Hohai University, Nanjing, China; Zili Dai from Department of Civil Engineering, Shanghai University, Shanghai, China; Bei Zhang and Yu Huang from Department of Geotechnical Engineering, College of Civil Engineering, Tongji University, Shanghai, People's Republic of China

the flexible barriers because modelling their deformation is more complex compared to a non-deformable rigid barrier. A summary of the assessment criteria is given in Table 4.

3.3. Details of the participants

3.3.1. Demographics of the participants

Figure 4 shows a summary of the demographics of the nine teams that took part in the prediction exercise and the 250 participants of the symposium. Seven out of the nine teams that participated were from academia and the rest were from industry. Among them, three teams were from Europe (e.g., Austria and Italy) and the rest were from Asia (e.g., Hong Kong, People's Republic of China). Among the participants, 95%, 3%, and 2% were from Asia, Europe, and other regions, respectively.

(a)

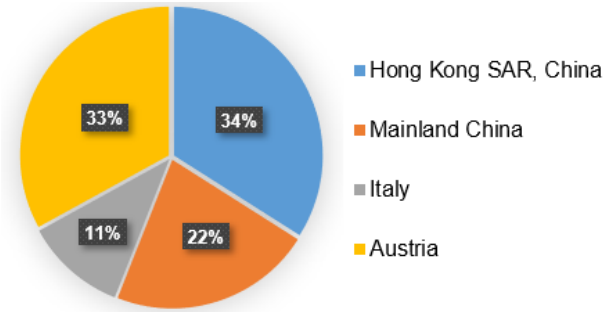

(b)

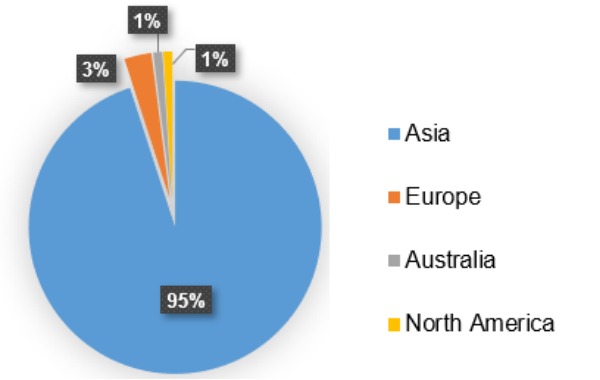

Figure 4. Demographics: (a) predictors; and (b) participants.

3.3.2. Prediction teams

Prediction teams used commercial and in-house numerical tools, and analytical equations to carry out their predictions. The numerical tools include the discrete element method (DEM), Material Point Method (MPM), Smoothed Particle Hydrodynamics (SPH), and finite element method (FEM). A summary of the models used by each team is given in Table 4.

4. Prediction results

This section compares the predicted and measured debris flow mobility and impact forces on dual rigid and flexible barriers. For each bar graph, the abscissa shows letters randomly assigned to each prediction team for anonymity. The ordinate shows the predicted values, which are normalised measured values. A normalised value of unity corresponds to that measured value. Predictions above and below unity represent over and underpredictions, respectively. Reference lines show the prediction bounds within 20% of the measured values. For engineering purposes, it is assumed that predictions within 20% of the measurements are reliable. The same graphical approach is used to describe the prediction values for other assessment parameters herein.

4.1. Debris flow mobility

Figure 5 shows a comparison of the predictions of the debris flow depths at an inclined distance of 3.45 m downstream from the gate before impacting the first barrier. Figure 5(a) shows the flow depth before impacting the first rigid barrier. It can be observed that, except for one prediction case (i.e., G), predicted values generally fall within 20% of the measured one. Predictions H and I are within 11% of the measured value. In contrast, prediction G is two times larger than that predicted. Generally, the results support the notion that existing numerical tools can provide close approximations of the flow depth before impact.

Figure 5(b) shows the flow depth before impacting the first flexible barrier. Only five predictions were submitted. All flow depths before impacting the flexible barrier are underpredicted. Prediction C exhibits the largest underprediction by 34%. It is expected that the flow depths before impacting the first rigid and flexible barriers should be identical because the flume conditions from the gate to the barrier location are the same. However, differences of up to 10% are observed for predictions A, D, and E. In particular, Prediction B exhibits a 30% shallower flow depth for the flexible barrier case compared to the rigid barrier one.

Figure 6 shows a comparison of the predicted frontal flow velocities at an inclined distance of 3.45 m downstream from the gate before impacting the first barrier. Figure 6(a) shows the predicted flow frontal velocities before impacting the first rigid barrier. Prediction C overpredicts the frontal flow velocity by 22% compared to that measured. The other eight predictions are within 20% of that measured. Only prediction G underpredicts the frontal flow velocity. Predictions D and E match the measured frontal flow velocity. Predictions A, B, F, H, and I overpredict the frontal flow velocity.

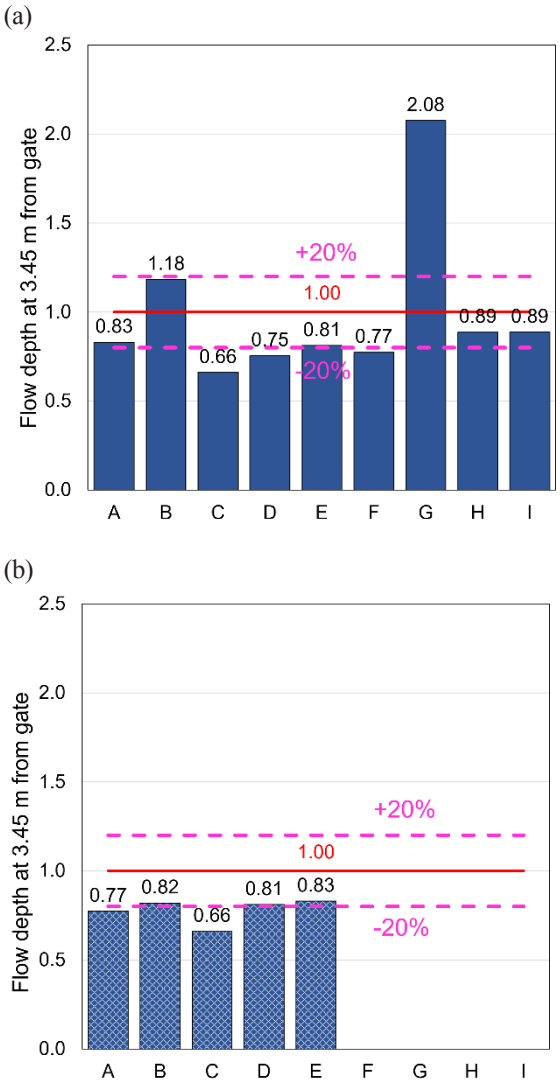

Figure 5. Comparison of flow depth before first (a) rigid; and (b) flexible barriers.

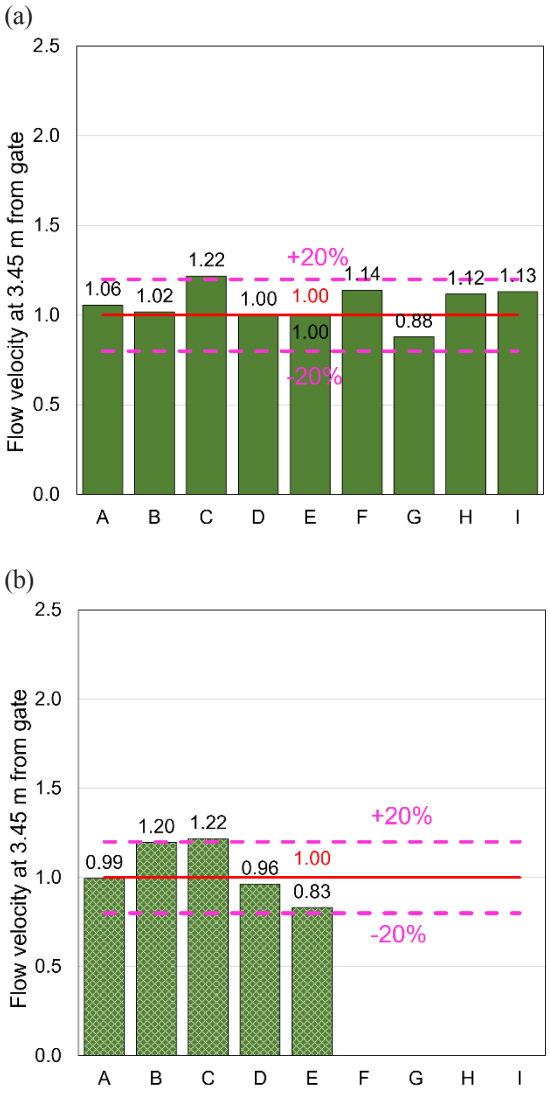

Figure 6. Comparison of flow velocity before first (a) rigid; and (b) flexible barriers.

Figure 6(b) shows a comparison of the predicted frontal flow velocities before impacting the flexible barrier. Only five predictions are made for the frontal velocities for the flexible barrier cases. Prediction C overpredicts the frontal flow velocity by 22% compared to that measured. The other prediction cases fall within 20% of the measured value. Predictions A and D are within 5% of the measured velocity. Moreover, it is expected that the frontal flow velocities before impacting the first rigid and flexible barriers should be identical because the flume conditions from the gate to the barrier location are the same. However, differences of up to 20% are observed for predictions A, B, D, and E. Prediction B exhibits an 18% increase in frontal flow velocity for the single flexible barrier case compared to the single rigid barrier case.

Eight out of the 14 flow depth predictions are within 20% of measured values. Twelve out of the 14 frontal flow velocity predictions are within 20% of measured values. Based on the flow depth and frontal velocity predictions before the first barriers, it can be assessed that existing numerical tools can reasonably predict the momentum of the flow, which is characterised by the product of the flow depth and velocity (Gray et al., 1999; Savage and Hutter, 1989), before impacting a barrier. Underpredictions of the flow depth or frontal flow velocity may be caused by difficulties in replicating dam-break initiation (Hogg and Pritchard, 2004; Kerswell, 2005) in the field-scale experiments or rheological models that cause the debris flow to spread to shallower flow depths (Laigle et al., 2003; Rickenmann et al., 2006). The flow depth and frontal flow velocity play an important role in the hydrostatic and hydrodynamic forces induced on a barrier, respectively (Albaba et al., 2018; Armanini, 1997; Armanini et al., 2020;

Faug, 2020). Therefore, underpredictions of the flow depth are expected to lead to underpredictions in the impact force.

4.2. Debris flow impact on the first barrier

Figure 7 shows a comparison of the predicted impact forces on the first rigid and flexible barrier to that measured. Impact forces predicted using existing design recommendations (GEO, 2020; Kwan and Cheung, 2012; Ng et al., 2021a) are shown for comparison. The 2-dimensional (2D) or 3-dimensional (3D) modelling approach utilised in the prediction exercise is indicated for each team. Although Prediction team F did not submit flow depth and velocity before impacting the flexible barrier, an impact force on the first flexible barrier was calculated by using an analytical approach.

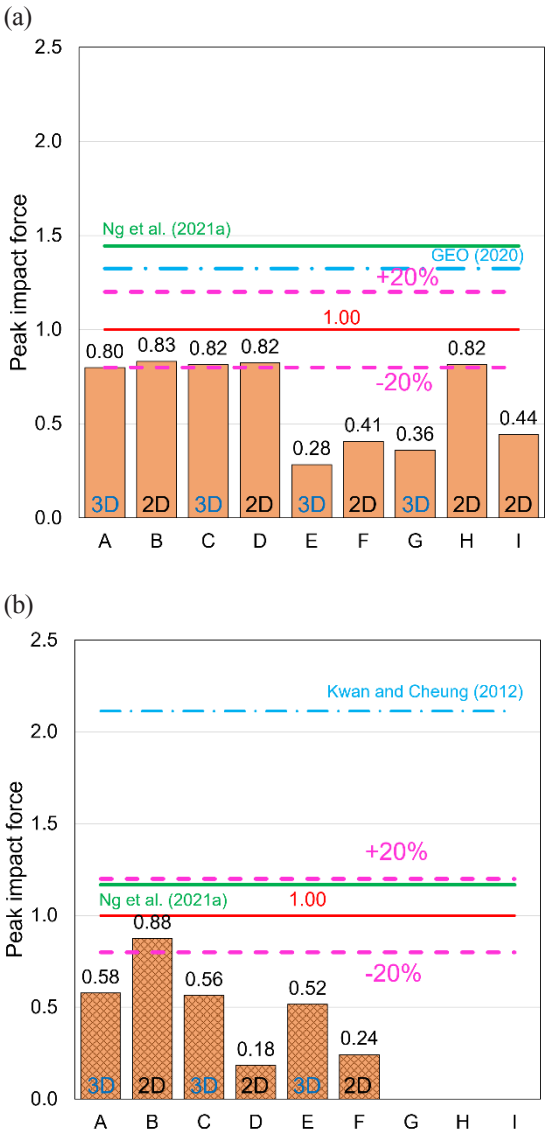

Figure 7. Comparison of impact force at first (a) rigid; and (b) flexible barriers.

Figure 7(a) shows a comparison of the predicted and measured impact forces on the first rigid barrier. All impact forces from the prediction teams are underpredicted. Predictions B and E underestimate the impact force by 17% and 72%, respectively. Five out of the nine predictions fall within 20% of the measured impact force on the first rigid barrier from which two teams use 3D models and three teams use 2D models. Compared to the calculated approaches, predictions are unable to provide conservative estimates of the impact force. The approach proposed by Ng et al. (2021a) overpredicts the impact force by 45%. The hydrodynamic approach for rigid barriers by GEO (2020) overpredicts the impact force by 32%. The calculated impact force by Ng et al. (2021a) is higher than that predicted using GEO (2020) because Ng et al. (2021a) additionally consider the hydrostatic force. It can be observed that a hydrodynamic impact coefficient of 1.5 is sufficient to predict the impact force induced on rigid barriers.

Figure 7(b) shows a comparison of the predicted and measured impact forces on the first flexible barrier. The peak impact force on the flexible barrier is underpredicted by all teams. Only one out of the six impact force predictions on the first flexible barrier is within 20% of the measured impact force. Notably, this prediction uses a 2D model. The approach proposed by Ng et al. (2021a) predicts an impact force that is 17% higher than that measured. In contrast, the approach proposed by Kwan and Cheung (2012) overpredicts the impact force by 110%. The difference between the calculated peak impact forces is because the approach by Ng et al. (2021a) adopts a hydrodynamic impact coefficient of unity while the approach proposed by Kwan and Cheung (2012) assumes a hydrodynamic impact coefficient of 2.0.

The predicted impact forces on the first rigid barrier except for case G are strongly correlated with the flow depth (Figure 5(a) and 5(b)) and flow velocity (Figure 6(a) and 6(b)), with the highest correlations for cases A, B, C, D and H. Furthermore, for case D, the underprediction of impact force for the flexible barrier is larger compared to the rigid barrier by up to 82%. This is because of the complexity of modelling the stiffness of the flexible barrier (Ng et al., 2020), especially using a 2D model. Except for case B, 3D models give closer predictions of impact force for flexible barriers compared with 2D models. However, the 3D model does not exhibit better performance in terms of estimating the impact force on the rigid barrier. This implies that the complex impact mechanisms of a debris flow on a flexible barrier require 3D modelling. The impact forces on the first barrier are underpredicted by all predictors for both rigid and flexible barriers. This suggests that existing numerical tools that are used generally underperform in the modelling of the complex interaction between the debris flow and barrier during impact.

Figure 8 shows a comparison of the predicted and measured runup heights on the first rigid barrier. An

additional reference line for calculated runup height (h_t) based on energy balance using Equation (4) is shown. Prediction F did not submit a runup height prediction for the first rigid barrier. The runup height is generally underestimated compared to that measured for all prediction cases. The runup height is related to the energy lost during the impact process and is indicative of whether the impact mechanism modelled is close to that observed in the field-scale experiments (Choi et al., 2015). Only the prediction H is within 20% of that measured. Although the flow depth (Figure 5) and frontal flow velocities (Figure 6) before impact were closely simulated, the impact forces (Figure 7(a)) and runup heights (Figure 8) are underestimated. This suggests that the modelled behaviour of the debris flow may be more dissipative compared to that of the field-scale experiments. The calculated runup height based on the conservation of energy also underpredicts the runup height by 25% because only a point mass is considered and the momentum flux from subsequent flow mass pushing the flow front upwards is not considered. The underpredicted runup heights indicate that further research is required to understand and elucidate the impact mechanisms. Although the flow velocity and flow depth before impact on the first barrier were closely predicted, underprediction of the runup height challenges the correct predictions of the impact process on subsequent barriers. This indicates that although models can obtain close predictions for some parameters, it does not necessarily mean that models can holistically capture the entire impact phenomena.

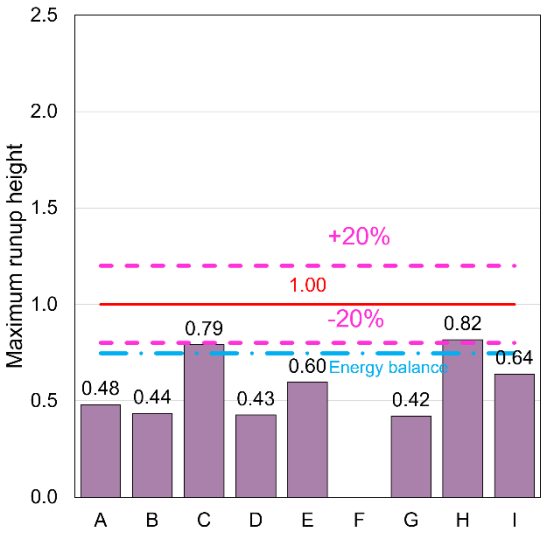

Figure 8. Comparison of maximum runup height at the first rigid barrier.

Figure 9 shows a comparison of the predicted and measured maximum deformation of the first flexible barrier. Only four prediction groups provided barrier deformations. All four predicted barrier maximum deformations underpredict the measured value. It is expected that underpredictions of the deformation should result in a higher impact force compared to that measured because of a stiffer barrier response. However, the impact force predicted on the first flexible barrier for all prediction cases was underestimated regardless of the 2D or the 3D modelling procedure used. More interestingly, none of the deformation prediction results are within 20% of the measured value. This highlights that there is a modelling mismatch between the deformation of the simulated barriers and the barrier impact. Evidently, the existing numerical tools are deficient in modelling the internal frictional dissipation of the flow interacting with the deformed barriers in order to obtain accurate barrier responses (Ng et al., 2020).

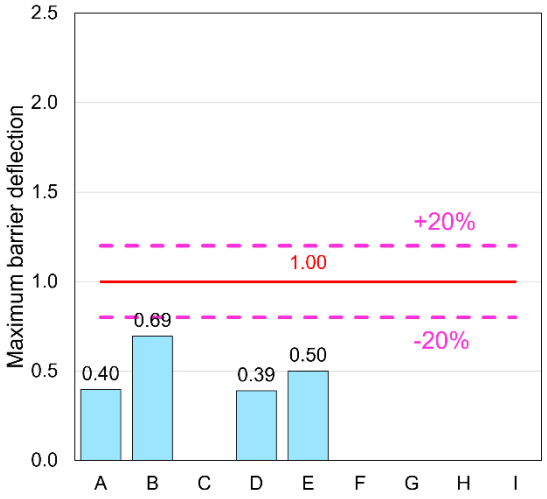

Figure 9. Comparison of maximum barrier deflection at the first flexible barrier.

4.3. Dynamics of debris overflow atop the first barrier

Figure 10 shows a comparison of the predicted overflow distance from the first barrier compared to that measured.

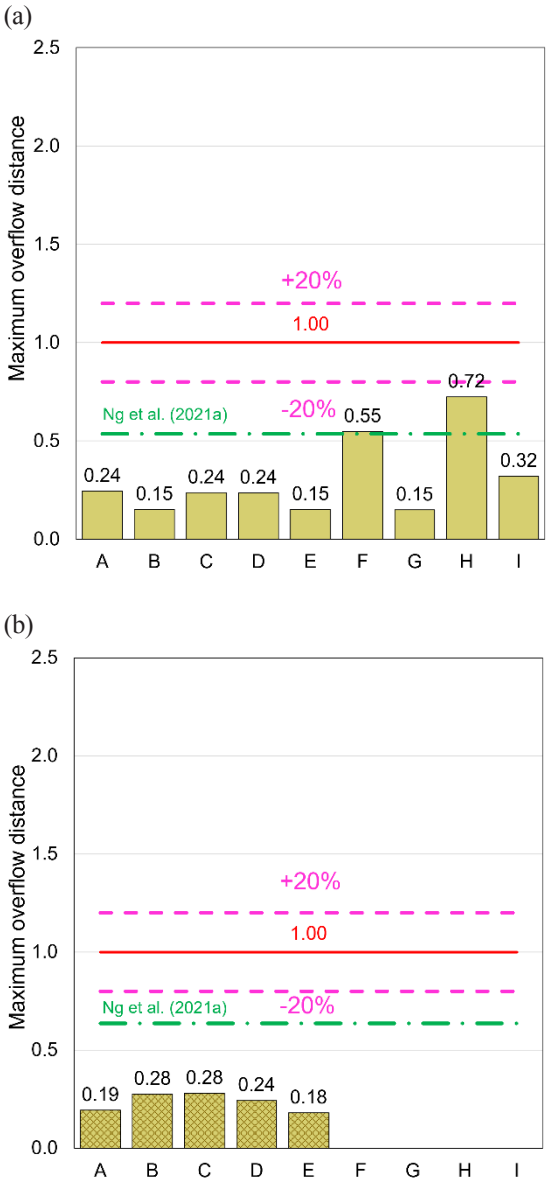

Figure 10. Comparison of maximum overflow distance for dual (a) rigid; and (b) flexible barriers.

Figure 10(a) shows a comparison of the results for the predicted overflow distances from the first rigid barrier. It can be seen that the overflow distances are underpredicted compared to that measured. None of the predictions are within 20% of the measured value. In addition, the approach proposed by Ng et al. (2021a) (i.e., Equation (6)) also underpredicts the overflow distance by 46%. This underprediction might be due to the assumptions of point mass and horizontal overflow launch angle.

This underprediction of the overflow distance is because Ng et al. (2021a) do not consider energy dissipation during flow-barrier interaction. The study also does not consider the overflow launch angle and assumes a horizontal overflow direction. Furthermore, a point mass approach to model a debris flow yields lower overflow distances because the momentum flux of incoming debris material is ignored.

Figure 10(b) shows a comparison of the results between predicted and measured overflow distances from the first flexible barrier. All overflow distances are underpredicted. The closest predictions (i.e., B and C) both underpredict the overflow distance by up to 72%. Moreover, the analytical approach proposed by Ng et al. (2021a) underpredicts the overflow distance by 36%. In contrast to the value calculated by Ng et al. (2021a) for the rigid barrier case, a lower underprediction is observed for the flexible barrier.

In the numerical models used for the Class A predictions, the overflow distance evolves with the momentum of the incoming debris flow. Debris overflow occurs continuously after flow runup at the first barrier. With an underprediction of flexible barrier deformation (Figure 9), it is unlikely that the flow runup and subsequent overflow processes are correctly captured by the numerical models. The underpredictions of overflow distance in flexible barriers are most likely a by-product of the dissipative behaviour of the modelled flow. Research to improve debris constitutive models and implementation of appropriate boundary conditions is warranted to improve the modelling of flow-barrier interaction.

Figure 11 shows a comparison between the predicted and measured landing angles from the first barrier. Figure 11(a) shows a comparison of the predicted landing angles from the first rigid barrier. Both over and underpredictions are exhibited. Eight out of the nine predictions are within 20% of that measured. The closest predictions (i.e., A and B) exhibit a difference of only 5% compared to that measured.

Figure 11(b) shows a comparison of the predicted landing angles from the first flexible barrier. Only five predictions were provided for the flexible barrier case. Both over and underpredictions are exhibited. Three out of the five predictions are within 20% of that predicted. Prediction A is the same as the measured landing angle. The discrepancies in predicted landing angles are smaller in the case of the rigid barrier compared to the flexible barrier. In the case of rigid barrier, the runup travels along the surface of the barrier before launching downstream. Since the barrier geometry is known, the ballistic trajectory of a point mass projectile and its landing angle can be easily calculated for a given launch velocity. However, for the modelled flexible barriers, the change in curvature due to barrier deformations likely affected the launch as well as landing angles of debris flow (Vicari et al., 2022). A higher landing angle means that the flow momentum is dissipated more when the overflow impacts the channel bed (Ng et al., 2022). Therefore, improved predictions of impact force on downstream barriers require accurate predictions of the landing angle at preceding barriers.

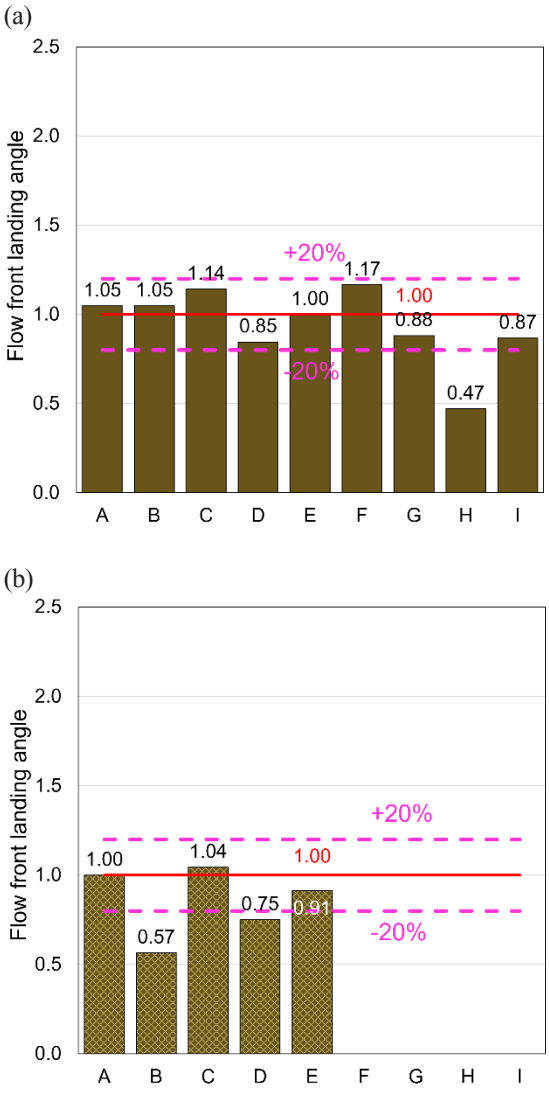

Figure 11. Comparison of flow front landing angle for dual (a) rigid; and (b) flexible barriers.

4.4. Debris flow impact on the second barrier

Figure 12 shows a comparison between predicted and measured peak impact forces on the second barrier. The peak impact forces calculated by using Equation (1) (GEO, 2020) and Equation (3) (Ng et al., 2021a) are shown for reference. The 2D or 3D modelling approach utilised in the prediction exercise is indicated for each team.

Figure 12(a) shows a comparison of the peak impact forces on the second rigid barrier. Both over and underpredictions of the peak impact force were reported. Only two predictions (i.e., D and H) are within 20% of the measured value. Interestingly, these two predictions use 2D modelling to achieve these close values which highlights that 2D modelling is sufficient to accurately model a rigid barrier response in relatively simple terrain. Six out of the nine predictions underestimate the impact force. Unlike the prediction results for the first rigid barrier, which are all underpredicted, three of the predicted impact forces on the second rigid barrier are overestimated. The calculated normalised impact force by using Equation (1) by GEO (2020) and Equation (3) by Ng et al. (2021a) overpredicts the impact force by 2.7 and 1.5 times, respectively. The approach proposed by Ng et al. (2021a) (i.e., Equation (3)) adopts a smaller hydrodynamic impact coefficient (α) for the second barrier compared to that used in the approach proposed by GEO (2020) (i.e., Equation (1)). The smaller α in the approach proposed by Ng et al. (2021a) (i.e., Equation (3)) considers the deceleration as well as partial retention of debris flow by the first barrier. Additionally, the approach proposed by Ng et al. (2021a) assumes that the flow depth impacting on the second barrier is the same as that on the first barrier, which allows conservative estimation of impact force on the second barrier.

Figure 12(b) shows a comparison between predicted and measured impact forces on the second flexible barrier. All of the peak impact forces are underpredicted. None of the predicted forces are within 20% of the measured value. The calculated normalised impact force using Equation (1) by Kwan and Cheung (2012) is higher by 4.5 times compared with measured values. The calculated normalised impact force using Equation (3) by Ng et al. (2021a) is only 1.3 times higher than the measured values. Similar to the closer prediction by Equation (3) in Figure 12(a) for the second rigid barrier, a closer prediction is achieved for the second flexible barrier by using Equation (3). This observation shows the importance of considering the dissipation of energy resulting from flow interaction with the upstream barriers prior to predicting the downstream barrier impact forces.

Moreover, a potential reason for the underestimation of the impact forces on the second barrier includes deficiencies in the rheological models adopted. It is expected that the first barrier may retain the soil in the debris flow and reduce its solid fraction. Consequently, the rheology of the debris flow impacting the first and second barriers is different.

Sophisticated numerical models may not always yield a better prediction of debris flow impact forces. A simple hydrodynamic equation (GEO, 2020) (i.e., Equation (2)) or an equivalent equation proposed by Ng et al. (2021a) (i.e., Equation (3)) gives consistent and safe predictions of the impact force on single and dual rigid and flexible barriers (Figure 7 and Figure 12). To err on the side of caution, an engineer should not be influenced by the sophistication of prediction techniques and instead appreciate that the basic techniques may provide consistent and conservative predictions of design impact force.

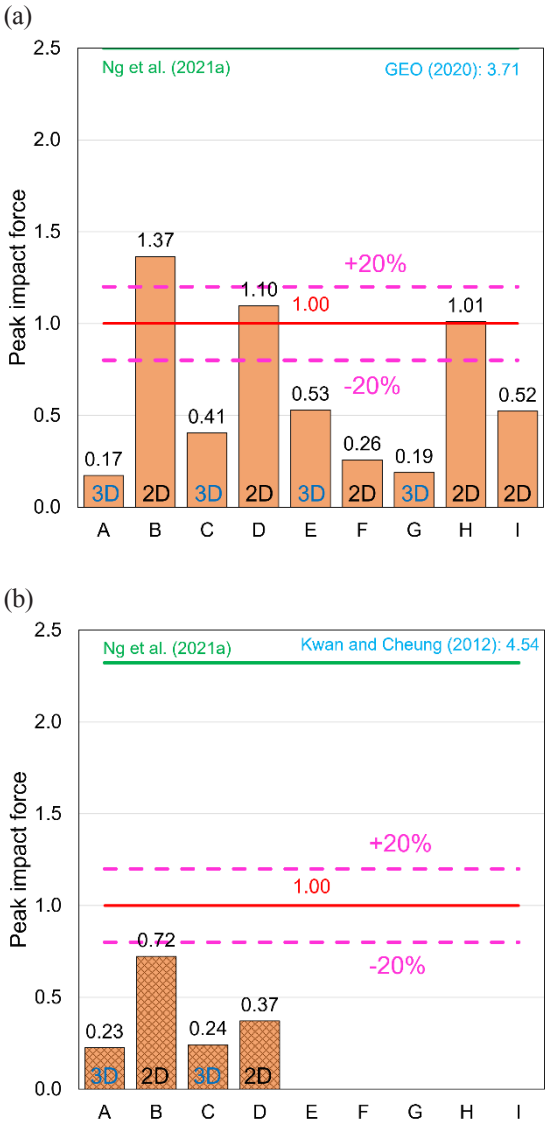

Figure 12. Comparison of peak impact force at the second (a) rigid; and (b) flexible barriers.

Figure 13 shows a comparison of the maximum runup heights on the second barrier. Equation (4) is used to calculate the runup height for reference. Figure 13(a) shows a comparison of the maximum runup heights on the second rigid barrier. It can be observed that the predicted runup height is underestimated for all prediction cases. In contrast, the calculated runup height from Equation (4) overpredicts the runup height by 24%. Compared to the runup prediction at the first barrier, runup at the second rigid barrier is underpredicted, which further reinforces the notion that simulated debris flows are more dissipative than the experiments. Figure 13(b) shows a comparison of the maximum runup heights on the second flexible barrier. It can be observed that the predicted runup height is underestimated for all prediction cases. In contrast, the calculated runup height from energy balance overpredicts the runup height by 1.2 times.

The underprediction of the overflow distance for the first barriers (Figure 10) might also have led to the underprediction of runup height at the second barrier for both rigid and flexible barrier cases. Underpredictions of overflow distance led to overpredictions of energy dissipation at flow-rigid bed interface which ultimately leads to underprediction of the runup height on the second barrier.

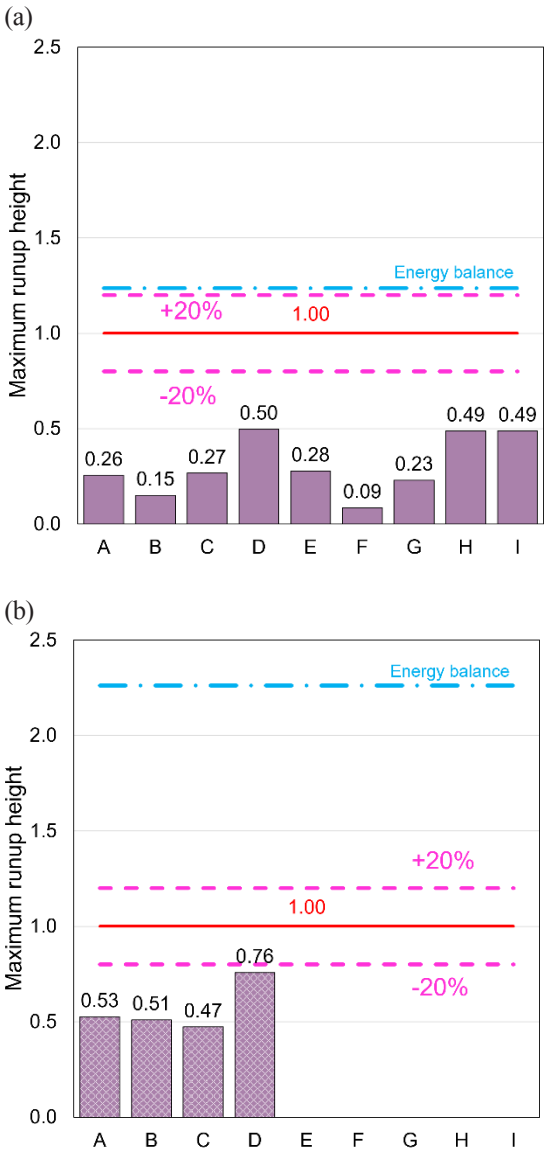

Figure 13. Comparison of maximum runup height at the second (a) rigid; and (b) flexible barriers.

5. Summary of Round-table Discussion

On the second day of the symposium, a roundtable discussion was organised. A summary of the discussion, including key observations, comments and future areas of required research put forward by the panellists and participants, is given below.

5.1. Debris flow rheology

Panellists agreed that although rheology is a fictitious concept, it enables engineers to simplify the complexities of modelling debris flow. It was evident from the prediction results that frictional rheology cannot capture the spatiotemporal heterogeneity of a debris flow, especially when it impacts a barrier. Most of the prediction teams adopted frictional rheology, which led to the underprediction of the impact forces. This suggests that the constitutive models adopted may be too dissipative. It is clear that further research is required to reveal the constitutive behaviour of a heterogonous solid-fluid mixture, especially the pore pressure changes.

5.2. 2D vs 3D models

Reasonable predictions were obtained from the 2D simulations in this prediction exercise. The panellists agreed that for simple geometries, such as a relatively uniform and straight channel, a 2D approximation of a flow-structure interaction may be sufficient. However, 3D modelling may be inevitable for more complex field cases and terrain. Debris flow impact is a complex process that likely requires the use of 3D models. With the advancement of computational capabilities, 3D models may not be as expensive to solve. Moreover, it was agreed that the complex impact mechanisms of a debris flow on a flexible barrier require 3D modelling.

5.3. Existing state of design practice

Current prediction results of debris flow impact force on the first barrier using flow velocity and flow depth at barrier locations are encouraging. However, after impact, the complicated mechanisms for runup, overflow and landing were largely not well captured. The panellists stressed the importance of analytical approaches for design. For multiple barrier designs, an analytical framework has been developed and verified by Ng et al. (2021a), which serves as a foundation for further development. Furthermore, the panellists acknowledged that predicting overflow and landing of debris flows still requires additional research in view of the prediction results in this symposium. Additionally, multiple barrier design guidelines should consider whether a barrier is cleaned after an impact event.

5.4. Erodible beds

The panellists acknowledged that the flume tests in this prediction symposium were conducted on non-erodible beds. As such, modelling the effects of erodible beds is a pressing scientific challenge that needs to be addressed. It was agreed that the flume or centrifuge models with non-erodible beds are a prerequisite to more complex boundary conditions. The panellists suggested the possibility of a future prediction exercise for debris flow entrainment models.

5.5. Full-scale test facilities

Currently, rock fall barriers are certified using standard testing procedures (EAD 340059-00-016, 2018). A similar standardisation would be beneficial for the design of flexible barriers for resisting debris flows. In practice, different proprietary products that use different mechanisms and designs are used in Hong Kong. A standardised test would simplify the design procedure leading to cost and time savings.

Foreseeable challenges for standardised tests include complexities involved in characterising the heterogeneous nature of debris flows. Furthermore, it was suggested that the 172 m-long flume in Kunming, China, which is under construction, may be used by designers to demonstrate the performance of a debris-resisting flexible barrier. In addition, such a unique facility enables the performance of individual components, such as brake elements, supporting cables and intercepting meshes, to be systematically evaluated.

6. Conclusions

Over recent years, significant advances have been made in the modelling of the dynamics between debris flows and single and dual rigid and flexible barriers. This paper summarised the state-of-the-art in flow-barrier interaction, details of the symposium, including the prediction cases, prediction results, and discussion from the roundtable discussion. Some key conclusions can be summarised as follows:

a) It is evident that most of the numerical results tend to underpredict the impact forces. Therefore, sophisticated numerical models for the prediction of debris flow impact dynamics may not always be better in terms of design applications. In contrast, Equation (3) provides conservative estimates for debris flow impact with the dynamic and static coefficients as (i) $\alpha = 1.5$ and $k = 1$ for the first rigid barrier (ii) $\alpha = 1$ and $k = 1$ for the second rigid barrier as well as dual flexible barriers. It should be noted that these design recommendations have only been validated by tests with a maximum debris flow volume of 9 m^3. As debris flow is scale-dependent, further validation with much larger flow volume is still warranted.

b) Existing numerical models remain far away from capturing realistic debris dynamics, including boulder inclusion and erodible beds, because these complex flow mechanisms are not well understood, let alone the impact dynamics on barriers. It is clear that more systematic

experimental evidence is needed. Owing to the scale-dependent behaviour of debris flows, the discipline urgently needs field-scale facilities that can produce high-fidelity data with well-controlled initial and boundary conditions to enable model evaluation. The unique 172 m-long flume that is under construction in Kunming, China, will be crucial for advancing the state-of-the-art modelling.

c) Despite the relatively good prediction of velocity and flow depth of debris flow prior to the first barrier impact, the subsequent impact and flow processes were not captured accurately. This was quite evident by the general underpredictions of the impact forces and runup heights on the first barrier and the overflow distances. It is clear that substantial research is still required to understand and elucidate the impact mechanisms, especially those on deformable flexible barriers.

Acknowledgements

The authors are grateful for the generous financial sponsorship from the Research Grants Council of the HKSAR Government, People's Republic of China (Project no.: AoE/E-603/18) and the Research Grants Council of Norway (Project no.: RCN21EG01). This paper is published with the permission of the Director of the Civil Engineering and Development, HKSAR Government . Sunil Poudyal, Aastha Bhatta and W A Roanga K De Silva gratefully acknowledge the support of the Hong Kong PhD Fellowship scheme (HKPFS) provided by the RGC of the HKSAR Government.

Notes on contributors

Ir Prof Charles W W Ng is currently the CLP Holdings Professor of Sustainability, Chair Professor in the Department of Civil and Environmental Engineering and Dean of Fok Ying Tung Graduate School at The Hong Kong University of Science and Technology (HKUST). He is also the Vice-President of The Hong Kong University of Science and Technology (Guangzhou) for Graduate Support. He is the immediate past president of International Society for Soil Mechanics and Geotechnical Engineering. He obtained his Ph.D. degree from the University of Bristol in 1993. After carrying out a period of post-doctoral research at the University of Cambridge between 1993 and 1995, he returned to Hong Kong and joined the HKUST as an Assistant Professor in 1995 and rose through the ranks to become a Chair Professor in 2011. Ir Prof Ng was elected as an Overseas Fellow at Churchill College, Cambridge University, in 2005 and was elected as a Changjiang Scholar (Chair Professor in Geotechnical Engineering) by the Ministry of Education in the Mainland China in 2010. He is a Fellow of the Institution of Civil Engineers (FICE), the American Society of Civil Engineers (FASCE), The Hong Kong Institution of Engineers (FHKIE), the Hong Kong Academy of Engineering Sciences (FHKEng) and the Royal Academy of Engineering (FREng). Ir Prof Ng has published more than 300 SCI journal articles and 230 conference papers and delivered more than 50 keynotes and state-of-the-art reports on five continents. He has supervised 66 Ph.D. and 59 MPhil students to graduation and mentored dozens of postdoctoral fellows and visiting scholars.

Prof Clarence E Choi is Assistant Professor of Civil Engineering at The University of Hong Kong (HKU). He obtained his Ph.D. from HKUST and his B.Sc. (with distinction) from the University of Calgary. He is the recipient of the Third Hutchinson Lecture (to be delivered in Oslo, Norway, in 2023) by the Federation of International Geo-Engineering Societies (FedIGS), Bright Spark Award by the International Society for Soil Mechanics and Geotechnical Engineering (ISSMGE) in 2021, Telford Premium Prize by the Institution of Civil Engineers (ICE), U.K., in 2017, R.M. Quigley Award by the Canadian Geotechnical Society (CGS) in 2017, Geotechnical Paper Award by the Hong Kong Institution of Engineers (HKIE) in 2022, Fugro Prize in 2015, and the Hong Kong Jockey Club Institute for Advanced Study Junior Fellowship from 2015 to 2019.

Dr Haiming Liu is a post-doctoral researcher in the Department of Civil and Environmental Engineering at The Hong Kong University of Science and Technology. He obtained his Ph.D. in Geotechnical Engineering from HKUST in 2019. His research interests lie in understanding the impact mechanisms of debris flow and developing novel structural countermeasures for debris flow mitigation.

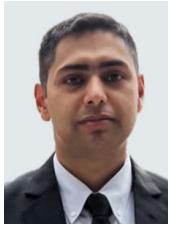

Mr Sunil Poudyal is a Ph.D. student in the Department of Civil and Environmental Engineering at The Hong Kong University of Science and Technology under the HK PhD Fellowship Scheme.

Ms Aastha Bhatta is a Ph.D. student in the Department of Civil and Environmental Engineering at The Hong Kong University of Science and Technology under the HK PhD Fellowship Scheme.

Ms W A Roanga K De Silva is a Ph.D. student in the Department of Civil and Environmental Engineering at The Hong Kong University of Science and Technology under the HK PhD Fellowship Scheme.

Ir Dr Raymond W M Cheung obtained his B.Sc. and M.Sc. degrees in Civil and Structural Engineering from The University of Hong Kong in the 1990s and Ph.D. from The Hong Kong University of Science and Technology in 2004. He is currently the Director of Geotechnical Engineering and Deputy Director of Mines of the Civil Engineering and Development Department, HKSAR Government, People's Republic of China.

References

[1] Albaba A, Lambert S and Faug T (2018). Dry granular avalanche impact force on a rigid wall: Analytic shock solution versus discrete element simulations. *Physical Review E*, 97, No. 5, 052903. 97(5), 052903.

[2] Armanini A (1997). On the dynamic impact of debris flows. In *Recent developments on debris flows* (Armanini A. and Michiue M (eds)). Springer, pp. 208-226.

[3] Armanini A, Rossi G and Larcher M (2020). Dynamic impact of a water and sediments surge against a rigid wall. *Journal of Hydraulic Research*, 58(2), pp. 314-325.

[4] ASI (2008) ONR 24801. In: *Protection Works for Torrent Control - Actions on Structures (Draft)*. Austria: Austrian Standard Institute, pp. 25.

[5] Bui HH, Fukagawa R, Sako K and Ohno S (2008). Lagrangian meshfree particles method (SPH) for large deformation and failure flows of geomaterial using elastic–plastic soil constitutive model. *International journal for numerical and analytical methods in geomechanics*, 32(12), pp.1537-1570.

[6] Bui HH, Fukagawa R, Sako K and Wells JC (2011). Slope stability analysis and discontinuous slope failure simulation by elasto-plastic smoothed particle hydrodynamics (SPH). *Géotechnique*, 61(7), pp. 565-574.

[7] CAGHP (2018). *Specification of design for debris flow prevention*. China: China Association of Geological Hazard Prevention.

[8] Chadwick A and Morfett J (1986). *Hydraulics in civil engineering*. Brighton Polytechnic.

[9] Choi CE, Au-Yeung SCH, Ng CWW and Song D (2015). Flume investigation of landslide granular debris and water runup mechanisms. *Géotechnique Letters*, 5(1), pp. 28-32.

[10] Cui Y, Cheng D, Choi CE, Jin W, Lei Y and Kargel JS (2019). The cost of rapid and haphazard urbanization: lessons learned from the Freetown landslide disaster. *Landslides*, 16(6), pp. 1167-1176.

[11] Cuomo S, Perna AD and Martinelli M (2021). Material point method (MPM) hydro-mechanical modelling of flows impacting rigid walls. *Canadian Geotechnical Journal*, 58(11), pp. 1730-1743.

[12] Dai Z, Huang Y, Cheng H and Xu Q (2017). SPH model for fluid–structure interaction and its application to debris flow impact estimation. *Landslides*, 14(3), pp. 917-928.

[13] Dávalos C, Cante J, Hernández JA and Oliver J (2015). On the numerical modeling of granular material flows via the particle finite element method (PFEM). *International Journal of Solids and Structures*, 71, pp. 99-125.

[14] Di Perna A, Cuomo S and Martinelli M (2022). Empirical formulation for debris flow impact and energy release. *Geoenvironmental Disasters*, 9(1), pp. 1-17.

[15] Dunatunga S and Kamrin K (2015). Continuum modelling and simulation of granular flows through their many phases. *Journal of Fluid Mechanics*, 779, pp. 483-513.

[16] EAD 340059-00-016 (2018) *European Assessment Document: Falling rock protection kits*. European Organization for Technical Assessment.

[17] ETAG027 (2013). *European Technical Assessment Guideline for Falling rock protection kits*. European Organization for Technical Assessment.

[18] Fang J, Wang L, Hong Y and Zhao J (2022). Influence of solid–fluid interaction on impact dynamics against rigid barrier: CFD–DEM modelling. *Géotechnique*, 72(5), pp. 391-406.

[19] Faug T (2015). Depth-averaged analytic solutions for free-surface granular flows impacting rigid walls down inclines. *Physical Review E*, 92(6), 062310.

[20] Faug T (2020). Impact force of granular flows on walls normal to the bottom: Slow versus fast impact dynamics. *Canadian Geotechnical Journal*, 58(1), pp. 114-124.

[21] Faug T, Caccamo P and Chanut B (2012). A scaling law for impact force of a granular avalanche flowing past a wall. *Geophysical Research Letters*, 39(23).

[22] Fraccarollo L and Capart H (2002). Riemann wave description of erosional dam-break flows. *Journal of Fluid Mechanics*, 461, pp. 183-228.

[23] GEO (2020) *GEO Technical Guidance Note No. 52 (TGN 52) Enhanced Technical Guidance on Design of Rigid Debris-resisting Barriers*. Hong Kong SAR, China: Geotechnical Engineering Office, Civil Engineering and Development Department, The Government of the Hong Kong Special Administrative Region, pp. 1-10.

[24] Geobrugg AG (2012). *Geobrugg: Protection systems for rockfall, debris flow, slope instability, mining, avalanche*. 8p.

[25] Gingold RA and Monaghan JJ (1977). Smoothed particle hydrodynamics: theory and application to non-spherical stars. *Monthly notices of the royal astronomical society*, 181(3), pp. 375-389.

[26] Gray JMNT, Wieland M and Hutter K (1999). Gravity-driven free surface flow of granular avalanches over complex basal topography. *Proceedings of the Royal Society of London. Series A: Mathematical, Physical and Engineering Sciences*, 455(1985), pp. 1841-1874.

[27] Hofmann R and Berger S (2022). Impacts of gravitational mass movements on protective Structures—Rock avalanches/granular flow. *Geosciences*, 12(6), 223.

[28] Hogg AJ and Pritchard D (2004). The effects of hydraulic resistance on dam-break and other shallow inertial flows. *Journal of Fluid Mechanics*, 501, pp. 179-212.

[29] Huang Y, Zhang W, Xu Q, Xie P and Hao L (2012). Run-out analysis of flow-like landslides triggered by the Ms 8.0 2008 Wenchuan earthquake using smoothed particle hydrodynamics. *Landslides*, 9(2), pp. 275-283.

[30] Hübl J and Fiebiger G (2005). Debris-flow mitigation measures. In *Debris-flow Hazards and Related Phenomena*. Berlin Heidelberg: Praxis Springer, pp. 445-487.

[31] Hübl J and Holzinger G (2003). Development of design basis for crest open structures for debris flow management in torrents: miniaturized tests for the efficiency estimation of debris flow breakers. *WLS Report*, 50.

[32] Hübl J, Suda J, Proske D, Kaitna R and Scheidl C (2009). Debris flow impact estimation. In: *Proceedings of the 11th international symposium on water management and hydraulic engineering*, Ohrid, Macedonia: 1, pp. 1-5.

[33] Hungr O and McClung DM (1987). An equation for calculating snow avalanche run-up against barriers. *National Research Council Canada, Institute for Research in Construction*.

[34] Iverson RM (2005). Regulation of landslide motion by dilatancy and pore pressure feedback. *Journal of Geophysical Research: Earth Surface*, 110(F2).

[35] Iverson RM (2015). Scaling and design of landslide and debris-flow experiments. *Geomorphology* 244, pp. 9-20.

[36] Iverson RM, George DL and Logan M (2016). Debris flow runup on vertical barriers and adverse slopes. *Journal of Geophysical Research: Earth Surface*, 121(12), pp. 2333-2357.

[37] Jin YF and Yin ZY (2022). Two-phase PFEM with stable nodal integration for large deformation hydromechanical coupled geotechnical problems. *Computer Methods in Applied Mechanics and Engineering*, 392, 114660.

[38] Jóhannesson T, Gauer P, Issler P and Lied K (Eds.) (2009). The Design of Avalanche Protection Dams, *Project Report EUR 23339*, Brussells: European Commission Directorate for Research.

[39] Kerswell RR (2005). Dam break with coulomb friction: A model for granular slumping. *Physics of Fluids*, 17, 057101.

[40] Kwan J (2012). *Supplementary technical guidance on design of rigid debris-resisting barriers (GEO Report, No. 270)*. Hong Kong SAR, China: Geotechnical Engineering Office, Civil Engineering and Development Department, The Government of the Hong Kong Special Administrative Region, pp. 1-91.

[41] Kwan JSH and Cheung RWM (2012) *Suggestions on design approaches for flexible debris-resisting barriers (Discussion Note No. DN 1/2012)*. Hong Kong SAR, China: Geotechnical Engineering Office, Civil Engineering and Development Department, The Government of the Hong Kong Special Administrative Region, pp. 1-90.

[42] Kwan JSH, Koo RCH and Lam C (2018) *Review on the Design of Rigid Debris-resisting Barriers (GEO Report, No. 339)*. Hong Kong SAR, China: Geotechnical Engineering Office, Civil Engineering and Development Department, The Government of the Hong Kong Special Administrative Region. pp 1-33.

[43] Kwan JSH, Koo RCH and Ng CWW (2015). Landslide mobility analysis for design of multiple debris-resisting barriers. *Canadian Geotechnical Journal*, 52(9), pp. 1345-1359.

[44] Kwan JSH, Sze EHY and Lam C (2019). Finite element analysis for rockfall and debris flow mitigation works. *Canadian Geotechnical Journal*, 56(9), pp. 1225-1250.

[45] Kwan JSH, Sze EHY, Lam C, Law RP and Koo RCH (2021). Development and applications of debris mobility models in Hong Kong. *Proceedings of the Institution of Civil Engineers-Geotechnical Engineering*, 174(5), pp. 593-610.

[46] Laigle D, Hector AF, Hübl J and Rickenmann D (2003). *Comparison of numerical simulation of muddy debris-flow spreading to records of real events*. In: 3rd International conference: debris-flow hazards mitigation: mechanics prediction and assessment, Davos, CHE, pp. 635-646

[47] Lambe TW (1973) Predictions in soil engineering. *Géotechnique*, 23(2), pp. 151-202.

[48] Larese A, Rossi R, Oñate E and Idelsohn SR (2008). Validation of the particle finite element method (PFEM) for simulation of free surface flows, *Engineering Computations*, 25(4), pp. 385-425.

[49] Leonardi A, Wittel F K, Mendoza M, Vetter R and Herrmann HJ (2016). Particle–fluid–structure interaction for debris flow impact on flexible barriers. *Computer-Aided Civil and Infrastructure Engineering*, 31(5), pp. 323-333.

[50] Li J, Cao Z, Hu K, Pender G and Liu Q (2018). A depth-averaged two-phase model for debris flows over erodible beds. *Earth Surface Processes and Landforms*, 43(4), pp. 817-839.

[51] Li X, Zhao J and Kwan JS (2020). Assessing debris flow impact on flexible ring net barrier: A coupled CFD-DEM study. *Computers and Geotechnics*, 128, 103850.

[52] Lichtenhahn C (1973). Die Berechnung von Sperren in Beton und Eisen- beton, Kolloquium on Torrent Dams, Heft, Mitteilungender Forstlichen Bundensanstalt Wien, 91–127. (In German)

[53] Lucy LB (1977). A Numerical Approach to the Testing of the Fission Hypothesis. *The Astronomical Journal*, 82, pp. 1013-1024.

[54] Maccaferri (2021). *Rockfall protection and snow barriers. Product Catalogue*. Available at: <https://www.maccaferri.com/in/download/brochure-in-rockfall-protection-and-snow-barriers-jan16/> [Accessed on 6th July 2022]

[55] Martinelli M and Galavi V (2022). An explicit coupled MPM formulation to simulate penetration problems in soils using quadrilateral elements. *Computers and Geotechnics*, 145, 104697.

[56] McDougall S and Hungr O (2005). Dynamic modelling of entrainment in rapid landslides. *Canadian Geotechnical Journal*, 42(5), pp. 1437-1448.

[57] MLR (2006). *Specification of geological investigation for debris flow stabilization*. China: Ministry of Land and Resources, pp. 1-31. (In Chinese)

[58] Nagl G, Hübl J and Kaitna R (2021). Measurements of velocity profiles in natural debris flows: a view behind the muddy curtain. *Environmental and Engineering Geoscience*, 27(1), pp. 87-94.

[59] Ng CWW, Choi CE, Koo RCH, Goodwin GR, Song D and Kwan JSH (2018). Dry granular flow interaction with dual-barrier systems. *Géotechnique*, 68(5), pp. 386-399.

[60] Ng CWW, Choi CE, Liu H, Poudyal S and Kwan JSH (2021a). *Design Recommendations for Single and Dual Debris Flow Barriers with and Without Basal Clearance*. In: Understanding and Reducing Landslide Disaster Risk: Volume 1 Sendai Landslide Partnerships and Kyoto Landslide Commitment (Sassa K., Mikoš M, Sassa S et al., (eds)). Springer International Publishing, Cham, pp. 33-53.

[61] Ng CWW, Liu H, Choi CE, Kwan JSH and Pun WK (2021b). Impact dynamics of boulder-enriched debris flow on a rigid barrier. *Journal of Geotechnical and Geoenvironmental Engineering*, 147(3), 04021004.

[62] Ng CWW, Majeed U and Choi CE (2022). Effects of solid fraction of saturated granular flows on overflow and landing mechanisms of rigid barriers. *Géotechnique*, pp. 1-41.

[63] Ng CWW, Song D, Choi CE, Liu LHD, Kwan JSH, Koo RCH and Pun WK (2017). Impact mechanisms of granular and viscous flows on rigid and flexible barriers. *Canadian Geotechnical Journal*, 54(2), pp. 188-206.

[64] Ng CWW, Wang C, Choi CE, De Silva WARK and Poudyal S (2020). Effects of barrier deformability on load reduction and energy dissipation of granular flow impact. *Computers and Geotechnics*, 121, 103445.

[65] NILIM (2007). Manual of technical standard for establishing Sabo master plan for debris flow and driftwood, technical note of NILIM no. 364. Tsukuba City, Japan: National Institute for Land and Infrastructure Management, Ministry of Land, Infrastructure and Transport. (In Japanese).

[66] NILIM (2016). Manual of Technical Standard for Designing Sabo Facilities Against Debris Flow and Driftwood. Technical Note of NILIM No. 905. Tsukuba City, Japan: National Institute for Land and Infrastructure Management, Ministry of Land, Infrastructure and Transport. (In Japanese).

[67] Pastor M, Haddad B, Sorbino G, Cuomo S and Drempetic V (2009). A depth-integrated, coupled SPH model for flow-like landslides and related phenomena. *International Journal for numerical and analytical methods in geomechanics*, 33(2), pp. 143-172.

[68] Peng C, Li S, Wu W, An H, Chen X, Ouyang C and Tang H (2022). On three-dimensional SPH modelling of large-scale landslides. *Canadian Geotechnical Journal*, 59(1), pp. 24-39.

[69] Peng C, Wang S, Wu W, Yu H, Wang C and Chen J (2019). LOQUAT: An open-source GPU-accelerated SPH solver for geotechnical modeling. *Acta Geotechnica*, 14(5), pp. 1269-1287.

[70] Peng C, Xu G, Wu W, Yu H and Wang C (2017). Multiphase SPH modeling of free surface flow in porous media with variable porosity. *Computers and Geotechnics*, 81, pp. 239-248.

[71] Pirulli M and Pastor M (2012). Numerical study on the entrainment of bed material into rapid landslides. *Geotechnique*, 62(11), pp. 959-972.

[72] Proske D, Suda J and Hübl J (2011). Debris flow impact estimation for breakers. *Georisk*, 5(2), pp. 143-155.

[73] Pudasaini SP and Fischer JT (2020). A mechanical erosion model for two-phase mass flows. *International Journal of Multiphase Flow*, 132, 103416.

[74] Ren D (2014) The devastating Zhouqu storm-triggered debris flow of August 2010: Likely causes and possible trends in a future warming climate, *Journal of Geophysical Research: Atmospheres*, 119, pp. 3643–3662.

[75] Rickenmann D, Laigle D, McArdell BW and Hübl J (2006). Comparison of 2D debris-flow simulation models with field events. *Computers and Geosciences*, 10(2), pp. 241-264.

[76] Savage SB and Hutter K (1989). The motion of a finite mass of material down a rough incline. *Journal of Fluid Mechanics*, pp. 177-215.

[77] Soga K, Alonso E, Yerro A, Kumar K and Bandara S (2016). Trends in large-deformation analysis of landslide mass movements with particular emphasis on the material point method. *Géotechnique*, 66(3), pp. 248-273.

[78] Song DR, Zhou GG, Choi CE and Zheng Y (2019). Debris flow impact on flexible barrier: effects of debris-barrier stiffness and flow aspect ratio. *Journal of Mountain Science*, 16(7), pp. 1629-1645.

[79] Song D, Chen X, Zhou GG, Lu X, Cheng G and Chen Q (2021). Impact dynamics of debris flow against rigid obstacle in laboratory experiments. *Engineering Geology*, 291, 106211.

[80] Stoffel M, Tiranti D and Huggel C (2014). Climate change impacts on mass movements—case studies from the European Alps. *Science of the Total Environment*, 493, pp. 1255-1266.

[81] SWCB (2019) *Soil and Water Conservation Handbook*. Taiwan: Soil and Water Conservation Bureau, pp. 523.

[82] Takahashi T (2014). *Debris Flow: Mechanics, Prediction and Countermeasures*, 2nd edition. Taylor and Francis Group.

[83] Tan D, Yin J, Feng W, Zhu Z, Qin J and Chen W (2020). New simple method for calculating impact force on flexible barrier considering partial muddy debris flow passing through. *Journal of Geotechnical and Geoenvironmental Engineering*, 145(9), 04019051.

[84] Trumer S (2015). *Handbook of rock fall protection systems*. Austria: Trumer Schutzbauten, pp. 1-10.

[85] Vagnon F (2020). Design of active debris flow mitigation measures: a comprehensive analysis of existing impact models. *Landslides*, 17(2), pp. 313-333.

[86] Vagnon F and Segalini A (2016). Debris flow impact estimation on a rigid barrier. *Natural Hazards and Earth System Sciences*, 16(7), pp. 1691-1697.

[87] Vandine DF (1996). *Debris Flow Control Structures for Forest Engineering*. British Columbia, Canada: Ministry of Forest Research Program.

[88] Vicari H, Ng CWW, Nordal S, Thakur V, De Silva WARK, Liu H and Choi CE (2022). The effects of upstream flexible barrier on the debris flow entrainment and impact dynamics on a terminal barrier. *Canadian Geotechnical Journal*, 59(6), pp. 1007-1019.

[89] Wang L, Zhang X, Lei Q, Panayides S and Tinti S (2022). A three-dimensional particle finite element model for simulating soil flow with elastoplasticity. *Acta Geotechnica*, pp. 1-15.

[90] Wendeler C, Volkwein A, Roth A, Herzog B, Hahlen N and Wenger M (2008) *Hazard prevention using flexible multi-level debris flow barrier*. In: INTERPRAEVENT Austria, pp. 547-554.

[91] Zhang W, Maeda K, Saito H, Li Z and Huang Y (2016). Numerical analysis on seepage failures of dike due to water level-up and rainfall using a water–soil-coupled smoothed particle hydrodynamics model. *Acta Geotechnica*, 11(6), pp. 1401-1418.